THz near-field imaging of biological tissues employing synchrotron radiation

Ulrich Schade[a], Karsten Holldack[a], Michael C. Martin[b], and Daniel Fried[c]

[a]Berliner Elektronenspeicherring-Gesellschaft für Synchrotronstrahlung mbH (BESSY), Albert-Einstein-Straße 15, 12489 Berlin, Germany;
[b]Advanced Light Source Division, Lawrence Berkeley National Laboratory, 1 Cyclotron Road, Berkeley, California 94720, USA;
[c]Division Biomaterials and Bioengineering, Department of Preventive and Restorative Dental Sciences, University of California, San Francisco, 707 Parnassus Ave., San Francisco, California 94143-0758, USA

ABSTRACT

Terahertz scanning near-field infrared microscopy (SNIM) below 1 THz is demonstrated. The near-field technique benefits from the broadband and highly brilliant coherent synchrotron radiation (CSR) from an electron storage ring and from a detection method based on locking on to the intrinsic time structure of the synchrotron radiation. The scanning microscope utilizes conical waveguides as near-field probes with apertures smaller than the wavelength. Different cone approaches have been investigated to obtain maximum transmittance. Together with a Martin-Puplett spectrometer the set-up enables spectroscopic mapping of the transmittance of samples well below the diffraction limit. Spatial resolution down to about $\lambda/40$ at 2 wavenumbers (0.06 THz) is derived from the transmittance spectra of the near-field probes. The potential of the technique is exemplified by imaging biological samples. Strongly absorbing living leaves have been imaged in transmittance with a spatial resolution of 130 μm at about 12 wavenumbers (0.36 THz). The THz near-field images reveal distinct structural differences of leaves from different plants investigated. The technique presented also allows spectral imaging of bulky organic tissues. Human teeth samples of various thicknesses have been imaged between 2 and 20 wavenumbers (between 0.06 and 0.6 THz). Regions of enamel and dentin within tooth samples are spatially and spectrally resolved, and buried caries lesions are imaged through both the outer enamel and into the underlying dentin.

Keywords: Terahertz, imaging, near-field microscopy, synchrotron radiation

1. INTRODUCTION

The terahertz (THz) and sub-THz region of the electromagnetic spectrum bridges the infrared and the microwave. This boundary region is beyond the normal reach of optical and electronic measurement techniques normally associated with these better-known neighbors. Only over the past decade has this THz region become scientifically accessible with broadband sources of moderate intensity being produced by ultra-fast laser pulses incident on biased semiconductors or non-linear crystals.[1,2]

Very recently, a much higher power source of THz radiation was demonstrated: coherent synchrotron radiation (CSR) from short, relativistic electron bunches.[3–5] Coherent synchrotron radiation will open up new territory in the THz frequency range with intensities many orders of magnitude higher than previous sources. The energy range between microwave and the far infrared, 3 - 33 cm^{-1} (0.1 - 1 THz), has proven to be challenging to access and is therefore referred to as the "THz gap". However, with the new CSR source at BESSY[3,5] we have been able to extend traditional infrared measurements down into this sub-terahertz frequency range.

The source is broad-band and is made up of longitudinally coherent single-cycle sub-picosecond pulses with a high repetition rate (100's of MHz). With the combination of high intensity and short pulse duration new opportunities for scientific research and applications are enabled across a diverse array of disciplines from condensed matter physics, to medical, technological, manufacturing, space and defense industries. Imaging, spectroscopy,

Further author information: U. Schade: E-mail: schade@bessy.de, Telephone: +49 30 6392-3449, www.iris.bessy.de

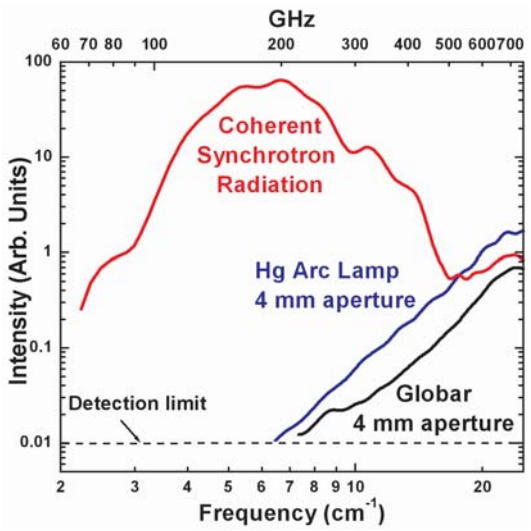

Figure 1. Measured far-IR intensity for the BESSY CSR source, compared to mercury arc and globar conventional thermal sources. While the turn-on of the CSR source below 2 cm^{-1} is a real effect of the CSR emission process, the drop off at the low frequency end is due to a combination of diffraction losses in the optical path of the beamline and the cutoffs of the optical components, such as the mylar beamsplitter, in the interferometer.

femtosecond dynamics, and driving novel non-linear processes are all among the potential applications. The high average power of the CSR source allows one to extend experimental conditions to lower frequencies than have been possible with thermal and conventional synchrotron sources (Fig. 1).

The spatial resolution of conventional THz imaging is diffraction limited and thus only features with a dimension from hundred micrometers to millimeters are resolvable. This limit can be overcome by utilizing near-field imaging techniques[6] achieving spatial resolutions of up to $\lambda/1000$.[7] However, extremely brilliant sources are necessary to compensate for intensity losses to confine the THz radiation at the cost of total power. In this paper, we make use of the stable CSR THz source at BESSY for scanning near-field microscopy in the THz and sub-THz range where spatial resolution below the diffraction limit is achieved on biological samples. Together with a Martin-Puplett spectrometer this technique also enables spectroscopic mapping of samples under investigation.

2. EXPERIMENTAL SET-UP

The THz scanning near-field imaging (SNIM) technique presented benefits from the broadband and highly brilliant CSR from the electron storage ring BESSY[3,5] utilizing a detection method based on locking onto the intrinsic time structure of the synchrotron radiation. The CSR source at BESSY is a pulsed source with a frequency of 1.25 MHz determined by the time the relativistic electron bunch needs to travel one orbit with a circumference of 240 m. The emitted CSR power varies with the square of the decaying electron ring current stored which has to be taken into account for data normalization. The THz SNIM is attached to the infrared beamline IRIS[8] at BESSY and the setup is shown in Fig. 2. The far-infrared port of the beamline provides a collimated CSR THz beam which is about 98 % linearly polarized. The THz beam passes through a Martin-Puplett spectrometer before being transferred to the SNIM where it is focused into a conical waveguide with a circular cross-section and an exit aperture of a diameter smaller than the wavelength. The sample is held in front of the exit aperture by a spring ensuring that the sample is in direct contact to the probe. Imaging is performed by moving the sample in front of the exit aperture by means of a computer controlled x-y stage. The evanescent field at the exit aperture penetrates the sample and the scattered radiation containing the spectral information is collected by an ellipsoidal mirror and is then focused onto a LHe-cooled InSb detector. The revolution frequency of the electron bunches stored is used as a reference for lock-in detection of the SNIM signal by a fast liquid

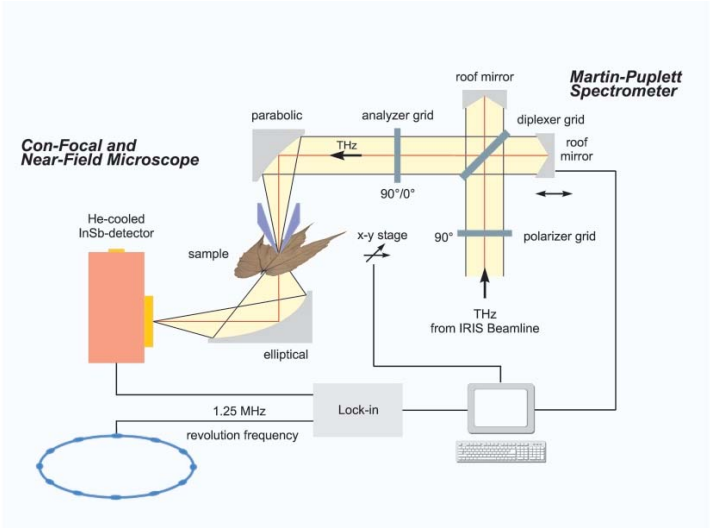

Figure 2. Schematic diagram of the THz scanning near-field infrared microscopy (SNIM) setup.

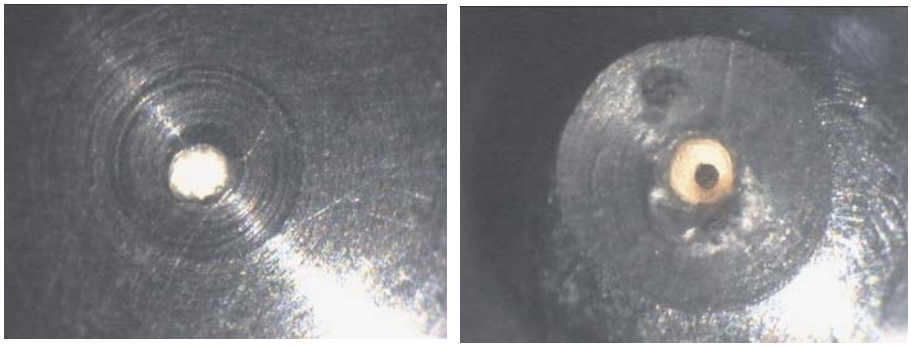

Figure 3. Aperture of 200 μm diameter with a coaxial wire of 80 μm thickness (right) and without a wire (left).

He cooled InSb detector. This detection provides a detection dynamics of nine orders of magnitude, which is essential for near-field imaging in strongly absorbing samples since it discriminates intensity from the source against thermal background radiation emitted by the beamline, the sample itself and the environment. The image is generated by interpretation of the SNIM signal versus sample position relative to the cone axis.

Conical aperture probes with a cone angle of 50° with two different aperture diameters of 100 and 200 μm have been employed for our experiments. Similar near-field probes have been proposed by Keilmann.[9] The conical aperture probe drastically attenuates the free-space THz radiation for wavelengths longer then the cut-off wavelength, $\lambda_c = 1.71\ d_c$, where d_c is the relevant cross-section diameter of the cone.[10] The power output of the near-field probe for a specific wavelength then depends on the cone angle and the diameter of the exit aperture.[11]

To increase the transmitted power and to shift the transmittance to longer wavelengths we also tested coaxial wire cones as described by Keilmann[10] and which are known to have theoretically no cut-off behavior. Both apertures under investigation, with and without a coaxial wire, are shown in Fig. 3. Fig. 4 shows the single channel spectra of the incident THz beam and the THz beam transmitted through the cones. Since the measurements are performed at ambient atmosphere all single channel spectra presented show distinct water absorption bands which do not interfere with our discussion. As expected from the geometry of the cones the transmitted power is reduced by several orders of magnitude. The transmittance of the cone without the wire

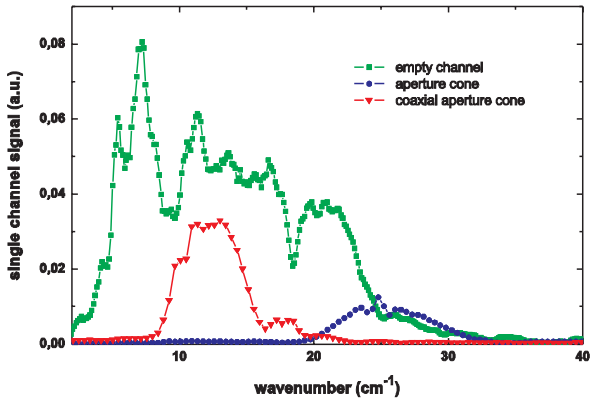

Figure 4. Single channel spectra of the empty spectrometer channel, of the aperture cone and of the coaxial aperture cone. The intensity of the empty channel spectra is attenuated by a factor of 100. Note, that the single channel intensities are shown in a linear scale. Intensities through both cones are for wavenumbers down to 2 cm^{-1}.

has its maximum in the higher frequency range at wavenumbers where the CSR source starts to emit radiation. For the coaxial cone with a wire also a cut-off is observed. However, the maximum transmission shifts to smaller wavenumbers, *i.e.* to longer wavelengths. In contrast to the cone without the wire the transmission is suppressed for larger wavenumbers, perhaps caused by an insufficient coupling of the plane wave to the cone in this frequency range.

The spatial resolution of the THz SNIM was investigated by scanning the edge of an aluminum film on a Si wafer along the near-field probe. We obtained a spatial resolution which is on the order of the diameter of the aperture. From the 2σ-value of the Gaussian fit of the first derivative of the experimental data, the spatial resolution is estimated to be about 130 μm for the 200 μm aperture probe and can be improved to 70 μm using the 100 μm aperture probe shown in Fig. 5. Taking broad band near-field images the spectral center of gravity at around 12 cm^{-1} is transmitted yielding an average spatial resolution of $\lambda/6$ for the 200 μm aperture and $\lambda/12$ for the 100 μm aperture, respectively.

3. INITIAL BIO-MEDICAL APPLICATIONS

The THz SNIM concept for applications on biological samples has been tested on leaves,[12] where the contrast is mostly formed by the amount of liquid water present. Recently, images of living leaves have also been obtained by other authors[13,14] from a confocal setup applying THz time-domain spectroscopy (TDS) to investigate the rehydration process of plants after watering. However, the spatial resolution of these investigations is restricted to the order of the wavelength applied. Using the THz SNIM technique presented here, much more detailed images can be obtained.

Fig. 6 shows a part of a freshly cut *parthenocissus* leaf imaged in transmission. In its THz near-field image an inner structure of the veins is apparent which is mainly formed by liquid water absorption and possible scattering at the structural boundaries. Both the THz image and the visible light image reveal similar object features but the THz SNIM enables studies of hydration dynamics with a high spatial resolution because it is sensitive to the water concentration in the sample.

As initial tests of the feasibility of using sub-THz radiation in dentistry for the diagnosis of tooth decay, we have imaged human tooth material using the THz SNIM together with the coherent synchrotron radiation source at BESSY. If caries lesions are detected early enough, they can be arrested without the need for surgical

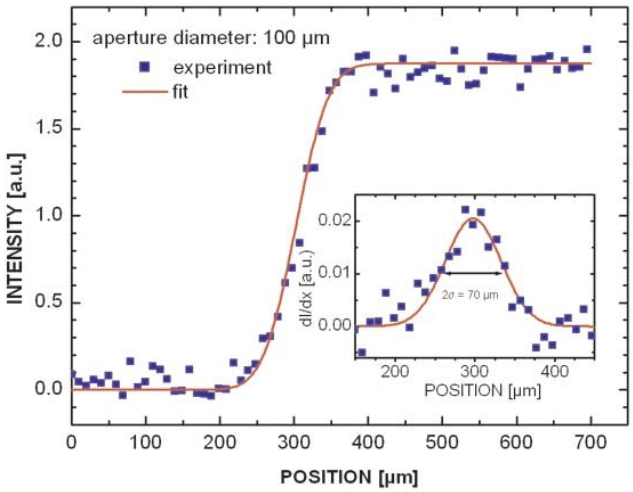

Figure 5. Measured and fitted spatial resolution curves for an exit aperture of 100 μm diameter. The inset shows a Gaussian fit of the first derivative of the measured curve used to determine the spatial resolution.

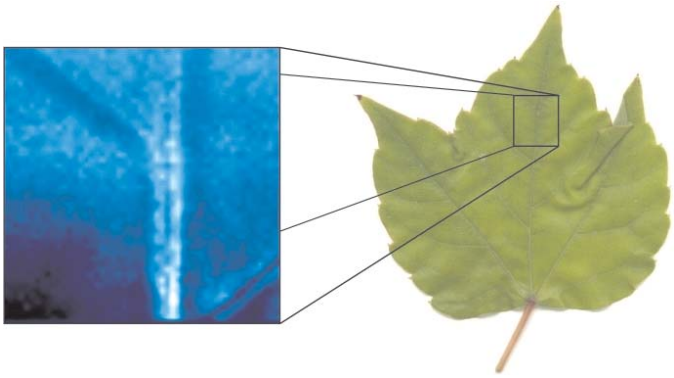

Figure 6. Near-field THz image (left) of a section of a *parthenocissus* leaf. Less absorption is indicated by a darker region in the THz image.

Figure 7. Photograph of a 2.7 m thick human tooth slab. The buried caries lesion is labeled on the left side.

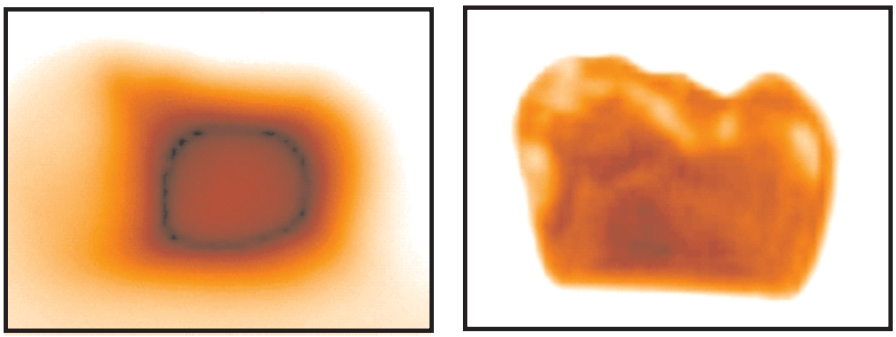

Figure 8. Confocal (left) and near-field (right) integral THz image of the tooth sample of Figure 12.

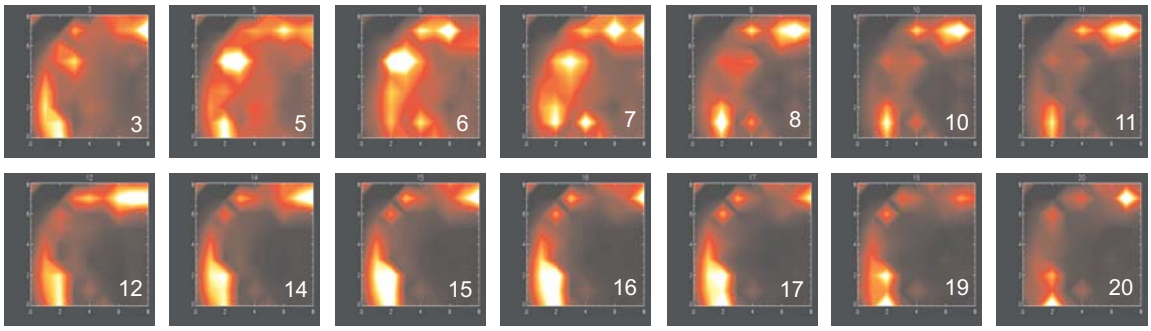

Figure 9. Series of spectral near-field images of the lesion region (upper left corner of the near-field image of Figure 12) between 3 and 20 cm^{-1} (between 0.5 and 3 mm wavelength). The corresponding wavenumber is indicated on the lower right corner of each spectral frame.

intervention. X-ray imaging is a well established method to image human teeth. With this method, buried caries lesions can be imaged by a contrast change due to demineralization in the particular tooth region. However, density contrast is weak for early demineralization and caries lesions are typically not visible in radiographs until the caries lesions have progressed much further and are more severely demineralized. Additionally, due to the ionizing nature of x-rays this method is not optimal for regular monitoring and many groups are exploring the infrared and THz radiation for medical imaging applications where both early diagnosis and safety issues are important. Recently, a more sensitive imaging method applying near infrared radiation was introduced,[15] showing the potential to image early dental decay in the enamel. Tooth decay in the dentin could not be imaged by this method since the dentin is almost opaque in the near infrared. THz pulse imaging in the far infrared wavelength range has been performed for the detection of early stage caries in the enamel layer of thin (100 μm) human tooth cross sections[16] obtaining a higher attenuation of THz radiation in carious enamel as compared with healthy enamel.

In contrast to the confocal imaging investigation mentioned above we applied the near-field technique and sub-THz radiation to image bulky tooth samples. Simulated buried caries lesions were produced by drilling 1-mm diameter cavity in the proximal region of the tooth and filling the cavity with hydroxyapatite paste[15] as shown in Fig. 7. The integral sub-THz image of the 2.7 mm thick tooth slab is shown in Fig. 8 both for con-focal imaging and near-field imaging. The near-field image was obtained utilizing the 200- μm wire cone while the confocal imaging was performed with the same optical set-up as shown in Fig. 7 except that the near-field cone was now removed. In confocal imaging geometry the tooth cannot be spatially resolved and the image is strongly blurred as one would expect from diffraction due to the long wavelengths involved. In contrast the enamel and the dentin regions of the tooth sample as well as the simulated buried caries lesion together with other inner structural diversities are spatially resolved in the near-field image. Spectral near-field images have been obtained from the

same sample. Fig. 14 shows a series of images of the area with the simulated lesion for different wavenumbers. In the spectral band between 5 and 7 wavenumbers (2., 3. and 4. frame from left of the upper row in Fig. 14) the lesion is indicated by a lower attenuation of the sub-THz radiation in comparison to the absorption of the surrounding material. Whether this experimentally observed contrast is indicative for buried carious lesions in human teeth is still speculative and further investigations on the optical properties of tooth tissues and on the propagation of sub-THz radiation in inhomogeneous bulky samples have to be conducted.

4. SUMMARY

The feasibility of using the stable, high power, coherent, broadband synchrotron radiation at sub-terahertz frequency at the electron storage ring BESSY for near-field spectroscopic experiments on biological samples is demonstrated. These results on confining sub-THz radiation from an electron storage ring presented may have important implications for extending near-field applications to other imaging or spectroscopic applications in both life and material sciences.

ACKNOWLEDGMENTS

The authors acknowledge support by D. Ponwitz, F. Höft (BESSY), K. Hinrichs, G. Hinte, and R. Herzlieb (ISAS).

REFERENCES

1. D. H. Auston, K. P. Cheung, J. A. Valdmanis, and D. A. Kleinman, "Cherenkov radiation from femtosecond optical pulses in electro-optic media," *Phys. Rev. Lett.* **53**, pp. 1555–1558, 1984.
2. B. Ferguson and X. C. Zhang, "Materials for terahertz science and technology," *Nature Materials* **1**, p. 254801, 2002.
3. M. Abo-Bakr, J. Feikes, K. Holldack, G. Wüstefeld, and H.-W. Hübers, "Steady-state far-infrared coherent synchrotron radiation detected at BESSY II," *Phys. Rev. Lett.* **88**, p. 254801, 2002.
4. G. L. Carr, M. C. Martin, W. R. McKinney, K. Jordan, G. R. Neil, and G. P. Williams, "High-power terahertz radiation from relativistic electrons," *Nature* **420**, pp. 153–156, 2002.
5. M. Abo-Bakr, J. Feikes, K. Holldack, P. Kuske, W. B. Peatman, U. Schade, G. Wüstefeld, and H.-W. Hübers, "Brilliant, coherent far-infrared (THz) synchrotron radiation," *Phys. Rev. Lett.* **90**, p. 094801, 2003.
6. B. Knoll and F. Keilmann, "Near-field probing of vibrational absorption for chemical microscopy," *Nature* **399**, pp. 134–137, 1999.
7. H. T. Chen, R. Kersting, and G. C. Cho, "Terahertz imaging with nanometer resolution," *Appl. Phys. Lett.* **83**, pp. 3009–3011, 2003.
8. U. Schade, A. Röseler, E. H. Korte, F. Bartl, K. P. Hofmann, T. Noll, and W. B. Peatman, "New infrared spectroscopic beamline at BESSY II," *Rev. Sci. Instrum.* **73**, pp. 1568–1570, 2002.
9. F. Keilmann, "Scanning tip for optical radiation," *U.S. Patent No. 14994818* , 1991 (filed 1989).
10. F. Keilmann, "FIR microscopy," *Infrared Phys. Technol.* **36**, pp. 217–224, 1995.
11. B. Knoll and F. Keilmann, "Electromagnetic fields in the cutoff regime of tapered metallic waveguides," *Opt. Commun.* **162**, pp. 177–181, 1999.
12. U. Schade, K. Holldack, P. Kuske, G. Wüstefeld, and H.-W. Hübers, "THz near-field imaging employing synchrotron radiation," *Appl. Phys. Lett.* **84**, pp. 1422–1424, 2004.
13. D. Mittelman, "Terahertz imaging," in *Sensing with Terahertz Radiation*, D. Mittelman, ed., pp. 117–153, Springer, Berlin, 2003.
14. M. Koch, "Bio-medical applications of THz imaging," in *Sensing with Terahertz Radiation*, D. Mittelman, ed., pp. 295–316, Springer, Berlin, 2003.
15. R. S. Jones, G. D. Huynh, G. J. Jones, and D. Fried, "Near-infrared transillumination at 1310-nm for the imaging of early dental decay," *Optics Express* **11**, pp. 2259–2265, 2003.
16. D. A. Crawley, C. Longbottom, B. E. Cole, C. M. Ciesla, D. Arnone, V. P. Wallace, and M. Pepper, "Terahertz pulse imaging: A pilot study of potential applications in dentistry," *Caries Research* **37**, pp. 352–359, 2003.